Rhenium-Oxo-Bis(acetylene) Anions: Structure, Properties, and Electronic Structure. Comparison of Re-O Bonding with That in Other Rhenium-Oxo Complexes[1]

Thomas R. Cundari*

Department of Chemistry, Memphis State University, Memphis, Tennessee 38152

Rebecca R. Conry, Esther Spaltenstein, Susan C. Critchlow, Keith A. Hall, Sam K. Tahmassebi, and James M. Mayer*,[2]

Department of Chemistry BG-10, University of Washington, Seattle, Washington 98195

Received August 2, 1993®

Reduction of $Re(O)I(RC{\equiv}CR)_2$ (**2**) or $[Re(O)(RC{\equiv}CR)_2]_2$ by two electrons gives $Re(O)(RC{\equiv}CR)_2Na$ (R = Me, **1a**; Et, **1b**; Ph, **1c**). Compounds **1** are unusual oxo complexes, being highly nucleophilic and strongly reducing. X-ray structures of **1a**·crypt and **1c**·2MeCN reveal $Re(O)(RC{\equiv}CR)_2$ units, as isolated anions in the former but, in the latter, connected via Na-O-Na bridges into centrosymmetric dimers. The acetylene ligands lie in a plane that is roughly perpendicular to the Re—O bond, but the C≡C vectors are splayed rather than parallel. The bond lengths and angles about rhenium are quite similar in the two structures, and quite close to the values found for **2** in which the splaying occurs to accommodate the iodide ligand. Reduction of **2a** to **1a**·crypt causes a lengthening of the Re-O bond from 1.697(3) to 1.745(7) Å and a drop in ν_{ReO} from 975 to 869 cm^{-1}, both indicative of a decrease in the Re-O bond order. The Re—C distances and C≡C stretching frequencies both decrease on reduction, indicating increased Re → acetylene back-bonding in **1**. Effective core potential calculations on $Re(O)(HC{\equiv}CH)_2^-$ (**A**), $Re(O)H(HC{\equiv}CH)_2$ (**B**), $Re(O)Cl_4^-$ (**C**), and $Re(O)F_5$ (**D**) have been performed with excellent agreement between the calculated structures and experimental crystallographic data (**A** and **B** are models for **1** and **2**). The Re-O bonds in the high-oxidation-state oxo complexes **C** and **D** follow the classical Ballhausen-Gray picture, with little mixing between the Re-O orbitals and orbitals on other ligands. In contrast, the frontier molecular orbitals in **A** and **B** exhibit significant delocalization over the rhenium, the oxygen, and the acetylene ligands. In **A**, the HOMO is an orbital largely Re $d_{x^2-y^2}$ in character, accounting for the high nucleophilicity at rhenium in **1**. The second-highest molecular orbital, only 0.8 eV below the HOMO, has significant Re-O π-antibonding and Re-acetylene π-back-bonding character, which provides a rationalization for the reduced Re-O bond order and strong back-bonding observed. There is also a ligand-based nonbonding orbital delocalized over the oxo and the acetylene ligands, as observed in other three-coordinate compounds involving acetylenes. Connections between the calculated electronic structure and the chemistry of **1** are emphasized.

Introduction

Transition metal oxo complexes have been an object of study, both experimental and theoretical, for many years.[3] Their importance as intermediates for biochemical (e.g., cytochrome P-450 enzymes[4]) and industrial (e.g., propylene to acrolein[5]) catalytic oxidation, as building blocks for advanced material oxides,[6] and as species in aqueous solution has contributed to much of the experimental and computational interest. The bonding in oxo compounds has been examined through a variety of computational and spectroscopic methods,[7] from the seminal work of Teltow,[7a] Wolfsberg-Helmholz,[7b] and Ballhausen-Gray[7c] to recent semiempirical studies,[7d,e] although systematic computational studies of coordinatively saturated oxo complexes at the *ab initio* level[7f] are surprisingly rare.

The overwhelming majority of oxo complexes contain transition metals with d electron counts of 0, 1, or 2. Species with higher d electron counts, such as d^4 iron-oxo porphyrin compounds[4] and ruthenium-oxo polypyridyl complexes,[8] are often highly reactive and transient com-

• Abstract published in *Advance ACS Abstracts*, December 1, 1993.

(1) Low-Valent Rhenium-Oxo Compounds. 14. Part 13: Reference 22.

(2) Presidential Young Investigator, 1988-1993.

(3) Extensive reviews of the literature of transition metal oxo compounds can be found in the following: (a) Holm, R. H. *Chem. Rev.* **1987**, *87*, 1401. (b) Griffith, W. P. *Coord. Chem. Rev.* **1970**, *5*, 459. (c) Nugent, W. A.; Mayer, J. M. *Metal-Ligand Multiple Bonds*; Wiley-Interscience: New York, 1988.

(4) *Cytochrome P-450*; Ortiz de Montellano, P. R., Ed.; Plenum: New York, 1986.

(5) Mitchell, P. C. H.; Trifiro, F. *J. Chem. Soc. A* **1970**, 3183.

(6) Bradley, D. C. *Chem. Rev.* **1989**, *89*, 1317. Caulton, K. G.; Hubert-Pfaltzgraf, L. G. *Chem. Rev.* **1990**, *90*, 969. Nandi, M.; Rhubright, D.; Sen, A. *Inorg. Chem.* **1990**, *29*, 3066.

(7) (a) Teltow, J. *Z. Phys. Chem.* **1938**, *B40*, 397; **1939**, *B43*, 198. (b) Wolfsberg, M.; Helmholz, L. *J. Chem. Phys.* **1952**, *20*, 837. (c) Ballhausen, C. J.; Gray, H. B. *Inorg. Chem.* **1962**, *1*, 111. (d) Representative examples: Du, P.; Axe, F. U.; Loew, G. H.; Canuto, S.; Zerner, M. C. *J. Am. Chem. Soc.* **1991**, *113*, 8614-21. Bursten, B. E.; Cayton, R. H. *Organometallics* **1987**, *6*, 2004-5; *Inorg. Chem.* **1989**, *28*, 2846-53. Tatsumi, K.; Hoffmann, R. *Inorg. Chem.* **1980**, *19*, 2656. Weber, J.; Garner, C. D. *Inorg. Chem.* **1980**, *19*, 2206-9. Brower, D. C.; Templeton, J. L.; Mingos, D. M. P. *J. Am. Chem. Soc.* **1987**, *109*, 5203-8. Miller, R. M.; Tinti, D. S.; Case, D. A. *Inorg. Chem.* **1989**, *28*, 2738-43. Deeth, R. J. *J. Chem. Soc., Dalton Trans.* **1991**, 1467. Green, J. C.; Guest, M. F.; Hillier, I. H.; Jarrett-Sprague, S. A.; Kaltsoyannis, N. *Inorg. Chem.* **1992**, *31*, 1588-94. (e) Cundari, T. R.; Drago, R. S. *Inorg. Chem.* **1990**, *29*, 487, 3904 and references therein. (f) See, for example: Ziegler, T.; Rauk, A.; Baerends, E. J. *Chem. Phys.* **1976**, *16*, 209-17. Goddard, W. A.; Rappé, A. K. *J. Am. Chem. Soc.* **1982**, *104*, 448.

0276-7333/94/2313-0322$04.50/0

plexes. Qualitative molecular orbital arguments[9] suggest that octahedral or square pyramidal oxo complexes with d^n, $n > 2$ are destabilized by population of orbitals which are metal $d\pi$–oxygen $p\pi$ antibonding, weakening the metal–oxo linkage and increasing $M^{\delta+}$–$O^{\delta-}$ polarization. As part of a continuing study of rhenium–oxo–acetylene complexes,[10-15] we reported the preparation and structure of $Re(O)(RC{\equiv}CR)_2^-$ anions (1), formally Re(I), d^6 species.[12] We suggested, on the basis of extended Hückel calculations and spectroscopic and crystallographic data, that there is some population of orbitals with Re–O π^* character in these complexes. This report provides both *ab initio* computational studies of the anions 1 and a full account of their syntheses and crystal structures. A study of the reactivity of 1 toward electrophiles and oxidants has appeared.[14] The chemistry of rhenium–imido–acetylene complexes, including analogs to compounds 1, has been the subject of a recent report.[16]

The primary goal of this study is to develop an understanding of the electronic structure of these unusual anions and how that electronic structure affects their molecular structure and reactivity. This work is part of continuing computational studies on the bonding, structure, and reactivity of multiply-bonded transition metal complexes using effective core potential (ECP) methods.[17] For comparison, we have also analyzed $Re(O)F_5$ (d^0),[18] $Re(O)Cl_4^-$ (d^2),[19] and $Re(O)H(HC{\equiv}CH)_2$ (formally d^4) oxo complexes. Previous work[17] has shown that the ECP methods employed herein can accurately predict structural and energetic properties for a wide variety of transition metal complexes. The wide range of formal oxidation states in the compounds analyzed here provides another interesting and challenging series for ECP methods.

Experimental Section

Syntheses were performed at ambient temperatures using standard Schlenk or vacuum line techniques and a continuous nitrogen flow glovebox except as indicated. Solvents and reagents were dried and deoxygenated by standard methods[20] unless otherwise mentioned. NMR spectra were obtained on Varian VXR-300 or Bruker WM-500 spectrometers. ^1H chemical shifts are reported in parts per million downfield from Me_4Si: δ (number of hydrogens, multiplicity, coupling constant, assignment). ^{13}C chemical shifts were referenced to solvent peaks (CD_3CN 0.5 ppm; CD_2Cl_2 55.0 ppm; C_6D_6 128.7 ppm). IR spectra were obtained on NaCl plates with Perkin-Elmer 283 or FT 1604 spectrometers and are reported in cm^{-1}. Elemental analyses were performed by Canadian Microanalytical (Delta, British Columbia). $Re(O)I(RC{\equiv}CR)_2$ [R = Me (**2a**), Et (**2b**),[10,21] Ph (**2c**)[22]] and $Re_2(O)_2(RC{\equiv}CR)_4$[13] were prepared as previously reported; other reagents were used as received.

$Re(O)(MeC{\equiv}CMe)_2Na$ (1a). To $Re_2O_2(MeC{\equiv}CMe)_4$ (1.017 g, 1.63 mmol), naphthalene (3 mg, 23 μmol, 1%), and freshly cut Na metal (0.425 g, 18.5 mmol, 6 equiv) was added 20 mL of THF. The solution was stirred for 2 h at ambient temperatures, over which time it turned dark orange. The excess Na was filtered off and the solvent removed *in vacuo*. A minimum amount (5–10 mL) of pentane was used to collect the brown-orange solid, 0.873 g (2.62 mmol, 80% based on Re). ^1H NMR (CD_3CN): 2.74 (s, $CH_3C{\equiv}CCH_3$). $^{13}C\{^1H\}$ NMR (C_6D_6): 19.9 ($CH_3C{\equiv}CCH_3$); 166.3 ($C{\equiv}C$). IR (Nujol): 1685 w ν(C≡C), 835, 805 ν(Re=O). Anal. Calcd for $C_8H_{12}NaORe$: C, 28.82; H, 3.63. Found: C, 28.47; H, 3.64.

[$Re(O)(MeC{\equiv}CMe)_2$][Na·crypt] (1a·crypt). A solution of 1a and the cryptand Kryptofix 222 (4,7,13,16,21,24-hexaoxa-1,10-diazabicyclo[8.8.8]hexacosane, Aldrich) in THF/Et_2O deposited dark crystals after standing in the drybox freezer at −10 °C for ca. 1 year. ^1H NMR (d_8-THF): 3.58 (s, 24H, crypt) 2.61 (t, 4 Hz, 8H, crypt), 2.66 (s, 12H, $CH_3C{\equiv}CCH_3$). IR (Nujol): 1675 w ν(C≡C), 1103 (s), 942, 869 (s) ν(Re=O).

$Re(O)(EtC{\equiv}CEt)_2Na$ (1b). Method A: $Re_2O_2(EtC{\equiv}CEt)_4$, Na, and Catalytic Naphthalene. To $Re_2O_2(EtC{\equiv}CEt)_4$ (0.777 g, 1.1 mmol), naphthalene (3 mg, 23 μmol, 2%), and 25 mL of THF was added 0.224 g of freshly cut Na metal (9.7 mmol, 9 equiv). The solution was stirred for 1.5 h at ambient temperature. The excess Na was filtered off, and the solvent was removed *in vacuo* to yield 0.838 g (2.2 mmol, 100% based on Re) of a dark orange viscous oil. **Method B: $Re(O)I(EtC{\equiv}CEt)_2$ and Na at −78 °C.** To a flask containing $Re(O)I(EtC{\equiv}CEt)_2$ (1.045 g, 2.1 mmol) and Na (0.333 g, 14.5 mmol, 7 equiv) at −78 °C was added 20 mL of THF. The reaction mixture was stirred for 5 h at −78 °C, becoming deep orange in color. The excess Na was filtered away, and the solvent was removed *in vacuo*. Diethyl ether (20 mL) was added and the mixture stirred intermittently at ambient temperature for 12 h. The precipitated NaI was filtered from the solution (0.291 g) and the solvent removed to yield **1b** as a dark orange oil slightly contaminated with NaI (0.787 g, ca. 1.9 mmol, 90%). ^1H NMR (CD_3CN): 1.23 (t, 7 Hz, 12 H, $CH_3CH_2C{\equiv}CCH_2CH_3$); 2.98, 3.04 (m, 4 H each, $CH_3CHH'C{\equiv}CCHH'CH_3$). $^{13}C\{^1H\}$ NMR (CD_3CN): 16.1 ($CH_3CH_2C{\equiv}CCH_2CH_3$); 27.9 ($CH_3CH_2C{\equiv}CCH_2CH_3$); 171.2 ($C{\equiv}C$). IR (neat): 1690 w ν (C≡C), 840, 810 ν(Re=O). IR (Nujol) plus 15-crown-5: 870, 859 ν(Re=O). Anal. Calcd for $C_{12}H_{20}ORENa_{1.2}I_{0.2}$: C, 34.35; H, 4.77. Found: C, 34.15; H, 4.63.

$Re(O)(PhC{\equiv}CPh)_2Na$ (1c). The synthesis was analogous to method B above, using 1.003 g (1.46 mmol) of $Re(O)I(PhC{\equiv}CPh)_2$, 0.20 g (8.9 mmol) of Na, and 25 mL of THF. The solution turned dark red-purple over the 3 h during which it was stirred at −78 °C. The NaI (0.211 g, 1.41 mmol, 96%) and dark purple 1c (0.826 g, 1.42 mmol, 97%) were collected. ^1H NMR

(8) (a) Dobson, J. C.; Seok, W. K.; Meyer, T. J. *Inorg. Chem.* **1986**, *25*, 1513. (b) Roecker, L.; Meyer, T. J. *J. Am. Chem. Soc.* **1987**, *109*, 746. (c) Roecker, L.; Dobson, J. C.; Vining, W. J.; Meyer, T. J. *Inorg. Chem.* **1987**, *26*, 779. (d) Thompson, M. S.; Meyer, T. J. *J. Am. Chem. Soc.* **1982**, *104*, 4106. (e) Dobson, J. C.; Helms, J. H.; Doppelt, P.; Sullivan, B. P.; Hatfield, W. E.; Meyer, T. J. *Inorg. Chem.* **1989**, *28*, 2200. (f) Sullivan, B. P.; Lumpkin, R. S.; Meyer, T. J. *Inorg. Chem.* **1987**, *26*, 1247.

(9) Mayer, J. M. *Comments Inorg. Chem.* **1988**, *8*, 125.

(10) Mayer, J. M.; Thorn, D. L.; Tulip, T. H. *J. Am. Chem. Soc.* **1985**, *107*, 7454–62.

(11) Spaltenstein, E.; Erikson, T. K. G.; Critchlow, S. C.; Mayer, J. M. *J. Am. Chem. Soc.* **1989**, *111*, 617–23.

(12) Spaltenstein, E.; Conry, R. R.; Critchlow, S. C.; Mayer, J. M. *J. Am. Chem. Soc.* **1989**, *111*, 8741–2.

(13) Spaltenstein, E.; Mayer, J. M. *J. Am. Chem. Soc.* **1991**, *113*, 7744–53.

(14) Conry, R. R.; Mayer, J. M. *Organometallics* **1991**, *10*, 3160–6.

(15) Tahmassebi, S. K.; Conry, R. R.; Mayer, J. M. *J. Am. Chem. Soc.* **1993**, *115*, 7553–7554.

(16) (a) Williams, D. S.; Schrock, R. R. *Organometallics* **1993**, *12*, 1148. (b) D. S. Williams, personal communication to T.R.C., 1993: in the drawing of the highest occupied b_2 orbital (the HOMO-1) in Figure 9 of this paper, the phase of the nitrogen p orbital should be reversed so that the Re–N interaction in this orbital is antibonding, analogous to the $3b_2$ orbital that is a focus here. This is confirmed by ECP and Fenske–Hall calculations on $Re(NH)(HCCH)_2^-$, Cundari, T. R., unpublished results.

(17) (a) Cundari, T. R. *Organometallics* **1993**, *12*, 1993. (b) Cundari, T. R. *J. Am. Chem. Soc.* **1992**, *114*, 10557. (c) Cundari, T. R. *J. Am. Chem. Soc.* **1992**, *114*, 7879. (d) Cundari, T. R.; Gordon, M. S. *J. Am. Chem. Soc.* **1993**, *115*, 4210. (e) Cundari, T. R. *Int. J. Quantum Chem., Proc. Sanibel Symp.* **1992**, *36*, 793. (f) Cundari, T. R.; Gordon, M. S. *J. Am. Chem. Soc.* **1991**, *113*, 5231. (g) Cundari, T. R.; Gordon, M. S. *Organometallics* **1992**, *11*, 55. (h) Cundari, T. R.; Gordon, M. S. *J. Am. Chem. Soc.* **1992**, *114*, 539. (i) Cundari, T. R.; Gordon, M. S. *J. Phys. Chem.* **1992**, *96*, 631. (j) Cundari, T. R.; Gordon, M. S. *Organometallics* **1992**, *11*, 3122.

(18) Alekseichuk, I. S.; Ugarov, V. V.; Sokolov, V. B.; Rambidi, N. G. *Zh. Struct. Khim.* **1981**, *22*, 795 quoted in Hagen, K.; Hobson, R. J.; Rice, D. A.; Trup, N. *J. Mol. Struct.* **1985**, *128*, 33.

(19) Lis, T.; Jezowska-Trzebiatowska, B. *Acta Crystallogr.* **1977**, *B33*, 1248.

(20) Perrin, D. D.; Armarego, W. L. F. *Purification of Laboratory Chemicals*, 3rd, ed.; Pergamon: New York, 1988.

(21) Manion, A. B.; Erikson, T. K. G.; Spaltenstein, E.; Mayer, J. M. *Organometallics* **1989**, *8*, 1871–3.

(22) Conry, R. R.; Mayer, J. M. *Organometallics* **1993**, *12*, 3179–3186.

Table 1. Atomic Coordinates (×10⁴) and Equivalent Isotropic Displacement Coefficients (Å² × 10³)[a] for [Re(O)(MeC≡CMe)₂][Na(crypt)] (1a·crypt)

	x	y	z	U_{eq}
Re(1)	1914(1)	2356(1)	2044(1)	49(1)
O(7)	1995(6)	1760(6)	3354(5)	67(2)
C(1)	633(8)	1666(8)	1504(7)	57(3)
C(2)	2512(14)	3847(8)	1364(9)	80(5)
C(3)	3519(11)	3151(10)	1106(9)	74(4)
C(4)	208(9)	2658(8)	1637(8)	60(3)
C(5)	2071(17)	5003(12)	1116(12)	114(7)
C(6)	4942(12)	3155(12)	485(13)	123(7)
C(7)	−789(14)	3463(11)	1386(12)	96(6)
C(8)	165(13)	696(9)	1145(11)	86(5)
Na(1)	4383(3)	7581(3)	3584(3)	51(1)
O(1)	5612(7)	9195(6)	2358(6)	70(3)
O(2)	3428(7)	8333(5)	2057(6)	66(2)
N(1)	7027(7)	7212(6)	2547(7)	58(3)
O(3)	5025(6)	5727(5)	2810(6)	65(3)
O(4)	2779(7)	5892(6)	4723(6)	70(3)
O(5)	3450(7)	8882(8)	5098(8)	85(3)
O(6)	5727(6)	7559(5)	4895(5)	58(2)
N(2)	1516(7)	7998(6)	4314(7)	62(3)
C(9)	1174(10)	8676(13)	5271(12)	95(6)
C(10)	2144(11)	9385(10)	5225(11)	86(5)
C(11)	1423(12)	6161(10)	5356(10)	86(5)
C(12)	3775(14)	8444(12)	6050(11)	101(6)
C(13)	6356(10)	5395(9)	2341(9)	74(4)
C(14)	7174(10)	6370(10)	1787(9)	76(4)
C(15)	5211(10)	8265(10)	5778(10)	74(4)
C(16)	2827(11)	5229(8)	3861(10)	73(4)
C(17)	4245(11)	4837(7)	3372(10)	74(4)
C(18)	786(9)	6985(8)	4692(9)	67(4)
C(19)	7566(10)	6827(9)	3487(9)	71(4)
C(20)	7091(9)	7564(9)	4467(10)	71(4)
C(21)	6715(11)	8921(12)	1441(10)	90(5)
C(22)	7631(9)	8210(8)	1885(10)	73(4)
C(23)	4628(12)	9917(8)	2070(9)	75(4)
C(24)	3895(12)	9374(8)	1468(10)	76(4)
C(25)	1206(10)	8583(10)	3351(10)	74(4)
C(26)	2056(11)	8141(9)	2287(10)	74(4)

[a] Equivalent isotropic U defined as $^1/_3$ of the trace of the orthogonalized U_{ij} tensor.

Table 2. Positional and Equivalent Isotropic Thermal Parameters for [Re(O)(PhC≡CPh)₂Na(MeCN)₂]₂ (1c·2MeCN)[a]

atom	x	y	z	B (Å²)
Re	0.28507(2)	0.10046(2)	0.38769(1)	3.170(4)
Na	0.43312(20)	−0.09208(19)	0.53454(12)	4.79(5)
O	0.3787(3)	0.0302(3)	0.4508(2)	4.50(9)
N1	0.3978(5)	−0.2762(5)	0.5174(4)	7.5(2)
N2	0.3149(6)	−0.0520(6)	0.6164(3)	8.2(2)
C1	0.3084(5)	0.1100(5)	0.2883(3)	3.7(1)
C2	0.2459(5)	0.0265(4)	0.2975(3)	3.6(1)
C3	0.1788(4)	0.2018(4)	0.4244(3)	3.4(1)
C4	0.2481(4)	0.2560(4)	0.3904(3)	3.4(1)
C11	0.3558(5)	0.1686(4)	0.2351(3)	3.9(1)
C12	0.4620(5)	0.2224(5)	0.2503(3)	4.8(1)
C13	0.5069(6)	0.2781(6)	0.2004(4)	6.2(2)
C14	0.4478(6)	0.2831(6)	0.1347(4)	6.8(2)
C15	0.3442(7)	0.2305(6)	0.1177(3)	6.8(2)
C16	0.2978(6)	0.1727(6)	0.1673(3)	5.4(2)
C21	0.1916(5)	−0.0670(4)	0.2622(3)	3.8(1)
C22	0.2195(6)	−0.1030(6)	0.2005(3)	5.8(2)
C23	0.1681(7)	−0.1927(6)	0.1689(3)	6.2(2)
C24	0.0865(6)	−0.2480(5)	0.1983(4)	5.8(2)
C25	0.0578(6)	−0.2134(5)	0.2595(4)	5.4(2)
C26	0.1106(5)	−0.1239(5)	0.2911(3)	4.5(1)
C31	0.0874(5)	0.2196(4)	0.4662(3)	3.5(1)
C32	0.0756(5)	0.3171(5)	0.4974(3)	4.8(1)
C33	−0.0097(6)	0.3344(6)	0.5373(3)	5.6(2)
C34	−0.0860(6)	0.2561(6)	0.5458(3)	5.6(2)
C35	−0.0782(5)	0.1597(5)	0.5153(3)	5.1(2)
C36	0.0088(5)	0.1413(5)	0.4757(3)	4.3(1)
C41	0.2612(5)	0.3639(4)	0.3652(3)	3.5(1)
C42	0.3681(5)	0.4027(5)	0.3547(3)	4.5(1)
C43	0.3781(6)	0.5074(6)	0.3335(4)	5.7(2)
C44	0.2824(7)	0.5719(5)	0.3225(4)	5.8(2)
C45	0.1753(6)	0.5336(5)	0.3318(3)	5.2(2)
C46	0.1651(5)	0.4323(5)	0.3532(3)	4.4(1)
C51	0.3704(6)	−0.3603(6)	0.5184(4)	5.7(2)
C52	0.3323(8)	−0.4679(6)	0.5219(4)	8.4(2)
C61	0.2523(6)	−0.0015(7)	0.6388(3)	6.1(2)
C62	0.1700(8)	0.0666(7)	0.6659(4)	8.0(2)

[a] Anisotropically refined atoms are given in the form of the isotropic equivalent thermal parameter defined as $^4/_3[a^2\beta_{11} + b^2\beta_{22} + c^2\beta_{33} + ab(\cos\gamma)\beta_{12} + ac(\cos\beta)\beta_{13} + bc(\cos\alpha)\beta_{23}]$.

(CD_3CN): 7.14 (t, 4 H, 8 Hz, H_{para}); 7.29 (t, 8 H, 8 Hz, H_{meta}); 7.67 (d, 8 H, 8 Hz, H_{ortho}). $^{13}C\{^1H\}$ NMR (CD_3CN): 126.6 (C_{para}); 128.4, 129.3 ($C_{ortho\ and\ meta}$); 141.5 (C_{ipso}); 172.2 (PhC≡*C*Ph). IR (Nujol): 1665 w ν(C≡C), 1591, 1305 w, 1276, 1154, 1069, 1025, 824 ν(Re═O), 755, 722, 690, 668; for 1c-^{18}O (prepared from Re(^{18}O)I(PhC≡CPh)$_2$[14]); 763 ν(Re═^{18}O). Anal. Calcd for $C_{28}H_{20}NaORe$: C, 57.82; H, 3.47. Found: C, 57.15; H, 4.26. **Re(O)(PhC≡CPh)₂Na·15-crown-5** (1c·15-crown-5) was prepared by method A with 0.101 g of $Re_2O_2(PhC{\equiv}CPh)_4$, 20 mg of Na, 3 mg of naphthalene, and 10 mL of THF. Then 15-crown-5 (28 μL, 0.14 mmol, 0.8 equiv; Aldrich) was added, the solution was concentrated by 50%, and pentane (20 mL) was added, giving a dark purple solid, which was washed twice. Yield: 0.105 g (0.098 mmol, 54%). ^{1}H NMR showed 2.2 equiv of crown per Re. IR (Nujol): 885 ν(Re═O).

X-ray Structure of [Re(O)(MeC≡CMe)₂][Na·crypt] (1a·crypt). An orange-brown crystal (dimensions 0.2 × 0.25 × 0.3 mm) was placed in a capillary under N_2 and mounted on an Enraf-Nonius CAD4 diffractometer (graphite-monochromatized Mo K_α radiation). Crystal data: triclinic, $P\bar{1}$, a = 10.623(2) Å, b = 12.410(2) Å, c = 12.442(2) Å, α = 84.13(1)°; β = 71.61(1)°; γ = 85.72(1)°, V = 1546.8(8) Å³, Z = 2, D_{calcd} = 1.524 g cm^{-3}. A total of 5759 reflections were collected ($2° \le 2\theta \le 50°$) at 295 K. The data were corrected for Lorentz and polarization effects, and for absorption using an empirical absorption method (μ = 3.89 mm^{-1}, transmission factors from 0.99 to 0.90), giving 5434 independent reflections (R_{int} = 1.3%), of which 4831 were observed reflections ($I > 4\sigma_I$). The structure was solved by direct methods (SHELX[23]). With all non-hydrogen atoms anisotropic and with hydrogen atoms fixed in calculated positions or located from a difference map and then regularized, final refinement of 335 parameters converged to R = 4.1%, R_w = 5.5%, and GOF = 1.05. Atomic coordinates and equivalent isotropic thermal parameters are given in Table 1; selected bond lengths and angles are given in Table 3.

X-ray Structure of [Re(O)(PhC≡CPh)₂Na·2CD₃CN]₂ (1c·2MeCN). Crystal data: monoclinic, $P2_1/c$, a = 11.640(2) Å, b = 12.648(2) Å, c = 19.668(4) Å, β = 71.61(1)°; V = 2858(2) Å³, Z = 4, D_{calcd} = 1.54 g cm^{-3}. Two octants of data (7179 reflections $2° \le 2\theta \le 55°$) were collected at 23 °C on a wedge-shaped crystal (dimensions 0.42 × 0.30 × 0.21 mm, mounted in a capillary under N_2) using an Enraf-Nonius CAD4 diffractometer. The data were corrected for Lorentz and polarization effects, for a 13.5% decay in intensity, and for absorption using an empirical absorption correction (μ = 4.347 mm^{-1}, transmission factors from 0.999 to 0.730), giving 4325 independent observed reflections ($I > 4\sigma_I$; R_{av} on F_o = 2.1%). The rhenium and sodium atoms were located on a Patterson map, and the structure was solved by subsequent least squares refinements and Fourier syntheses. With all 37 non-hydrogen atoms anisotropic and with hydrogen atoms placed in positions located from a difference map and regularized, final refinement of 334 parameters converged to R = 3.2%, R_w = 3.5, and GOF = 1.28. Atomic coordinates and equivalent isotropic thermal parameters are given in Table 2; selected bond lengths and angles are given in Table 3.

(23) Sheldrick, G. M. SHELX: Program for Crystal Structure Determination, University of Cambridge, 1978.

Table 3. Bond Lengths (Å) and Angles (deg) for [Re(O)(MeC≡CMe)$_2$][Na(crpyt)] (1a·crypt), [Re(O)(PhC≡CPh)$_2$Na(MeCN)$_2$]$_2$ (1c·2MeCN), and Re(O)I(MeC≡CMe)$_2$ (2a)[a]

1a·crypt		1c·2MeCN		2a[b]
Re(1)–O(7)	1.745(7)	Re–O	1.756(3)	1.697(3)
Re(1)–C(1)	1.976(10)	Re–C(2)	1.994(5)	2.066(5)
Re(1)–C(2)	2.014(10)	Re–C(4)	2.017(5)	2.038(5)
Re(1)–C(3)	1.999(11)	Re–C(3)	1.995(5)	2.061(5)
Re(1)–C(4)	2.030(10)	Re–C(1)	2.019(5)	2.040(5)
C(1)–C(4)	1.287(13)	C(1)–C(2)	1.312(7)	1.288(7)
C(2)–C(3)	1.302(17)	C(3)–C(4)	1.319(7)	1.278(7)
C(1)–C(8)	1.495(17)	C(2)–C(21)	1.462(7)	1.459(7)
C(2)–C(5)	1.508(18)	C(4)–C(41)	1.468(7)	1.494(7)
C(3)–C(6)	1.466(15)	C(3)–C(31)	1.461(7)	1.485(7)
C(4)–C(7)	1.485(18)	C(1)–C(11)	1.461(7)	1.470(7)
O(7)–Re(1)–C(1)	112.5(3)	O–Re–C(2)	114.8(2)	114.2(2)
O(7)–Re(1)–C(2)	125.4(5)	O–Re–C(4)	125.8(2)	109.1(2)
O(7)–Re(1)–C(3)	115.0(3)	O–Re–C(3)	114.8(2)	114.8(2)
O(7)–Re(1)–C(4)	124.4(3)	O–Re–C(1)	123.4(2)	108.8(2)
C(1)–Re(1)–C(2)	119.1(5)	C(2)–Re–C(4)	117.5(2)	117.6(2)
C(3)–Re(1)–C(4)	118.2(4)	C(1)–Re–C(3)	119.9(2)	117.3(2)
C(1)–Re(1)–C(3)	127.7(4)	C(2)–Re–C(3)	123.9(2)	130.5(2)
C(2)–Re(1)–C(4)	90.1(5)	C(1)–Re–C(4)	91.7(2)	88.3(2)
C(1)–C(4)–C(7)	141.2(12)	C(2)–C(1)–C(11)	142.0(5)	144.9(5)
C(4)–C(1)–C(8)	135.6(10)	C(1)–C(2)–C(21)	142.6(5)	144.0(5)
C(2)–C(3)–C(6)	138.0(12)	C(4)–C(3)–C(31)	139.8(5)	144.3(5)
C(3)–C(2)–C(5)	143.3(11)	C(3)–C(4)–C(41)	139.4(5)	145.8(5)
		O–Na	2.274(4)	
		O–Na′	2.301(4)	
		Na–N(1)	2.379(6)	
		Na–N(2)	2.335(7)	
		Re–O–Na	157.7(2)	
		Re–O–Na′	112.8(2)	
		Na–O–Na′	89.5(1)	
		O–Na–O′	90.5(1)	
		O–Na–N(1)	122.8(2)	
		O–Na–N(2)	103.0(2)	
		O′–Na–N(1)	119.3(2)	
		O′–Na–N(2)	119.6(2)	
		N(1)–Na–N(2)	101.7(3)	

[a] Each horizontal line corresponds to equivalent parameters in the three species. [b] Data for **2a** from ref 10.

Computational Methods

Calculations employed the quantum chemistry program GAMESS[24] in sequential (Memphis State University), vector (at the National Center for Supercomputing Applications), and parallel (Oak Ridge National Laboratories and San Diego Supercomputer Center) modes, the parallel implementation using up to 128 nodes on an iPSC/860. Effective core potentials[25] (ECPs) replace chemically less important core orbitals and make calculations feasible for all rows of the transition series, including the third-row transition metal complexes described here. Relativistic effects, which can be important in such heavy atoms, are also included in the derivation of the ECP scheme.[25] The ECPs and valence basis sets of Stevens *et al.*[25] are used for heavy atoms while hydrogen atoms are described with the -31G basis set. Basis sets for heavy main-group elements are augmented with a set of d polarization functions[26] The combination of ECPs, basis sets, and level of theory employed here has been successfully tested for a large number of multiply-bonded transition metal complexes.[17] Geometry optimization are done at the restricted Hartree–Fock (RHF) level for closed-shell singlets. Vibrational frequencies are calculated at stationary points to identify them as minima (all positive frequencies) or transision states (one imaginary frequency). Canonical RHF molecular orbitals were transformed to localized variants using the Pipek–Mezey algorithm.[27] Intrinsic stretching frequenices were calculated using the method of Boatz and Gordon.[28]

Scheme 1. Synthesis of NaRe(O)(RC≡CR)$_2$ (1)

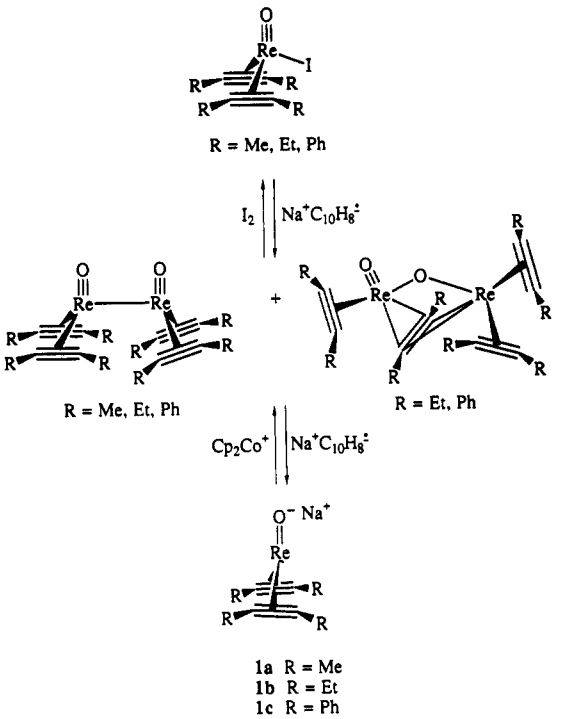

Results and Discussion

I. Experimental Studies. A. Syntheses and Properties. The reduction of Re(O)I(RC≡CR)$_2$ (**2**)[10] with 1 equiv of a reducing agent (e.g., sodium naphthalenide, $NaC_{10}H_8$, or $^tBu_2Zn$) results in loss of iodide and formation of rhenium–oxo dimers, $Re_2O_2(RC{\equiv}CR)_4$, as symmetric and asymmetric isomers (Scheme 1).[13,29] Two equivalents of sodium naphthalenide form monomeric rhenium–oxo anions as their sodium salts, NaRe(O)(RC≡CR)$_2$ (**1a**, R = Me; **1b**, R = Et; **1c**, R = Ph; Scheme 1).[12] Compounds **1** can also be formed by reduction of the dimers with 1 equiv of $NaC_{10}H_8$ per Re.

Clean isolation of the anions **1** by these routes is difficult, for two reasons. The anions formed under these conditions are very soluble even in nonpolar media such as pentane, preventing easy separation from the naphthalene byproduct. This solubility is presumably due to tight ion pairing between the sodium cations and the rhenium–oxo anions. Consistent with this, **1c** crystallizes from acetonitrile as a dimer, [Re(O)(PhC≡CPh)$_2$Na(MeCN)$_2$]$_2$ (**1c**·2MeCN), held together by sodium–oxygen interactions (see below). Reduction of Re(O)I(RC≡CR)$_2$ (**2**) yields **1** and 1 equiv of NaI, which is incorporated into the ion-paired clusters and therefore difficult to remove. Compounds **1** are much more soluble in pentane in the presence of NaI. This is

(24) (a) GAMESS (General Atomic and Molecular Electronic Structure System): Schmidt, M. W.; Baldridge, K. K.; Boatz, J. A.; Jensen, J. H.; Koseki, S.; Gordon, M. S.; Nguyen, K. A.; Windus, T. L.; Elbert, S. T. *QCPE Bull.* **1990**, *10*, 52. (b) Further discussion of the implementation of GAMESS to run on parallel architectures can be found in: Schmidt, M. W.; Baldridge, K. K.; Boatz, J. A.; Jensen, J. H.; Koseki, S.; Matsunaga, N.; Gordon, M. S.; Nguyen, K. A.; Su, S.; Windus, T. L.; Elbert, S. T.; Montgomery, J.; Dupuis, M. *J. Comput. Chem.* **1993**, *14*, 1347.

(25) Krauss, M.; Stevens, W. J.; Basch, H.; Jasien, P. G. *Can. J. Chem.* **1992**, *70*, 612.

(26) Pople, J. A.; Hehre, W. J.; Radom, L.; Schleyer, P. v. R. *Ab-Initio Molecular Orbital Theory*; Wiley: New York, 1986.

(27) Pipek, J.; Mezey, P. Z. *J. Chem. Phys.* **1989**, *90*, 4916.

(28) Boatz, J. A.; Gordon, M. S. *J. Phys. Chem.* **1989**, *93*, 1819.

(29) With 2-butyne ligands, reduction yields only the symmetric dimer $Re_2(O)_2(MeC{\equiv}CMe)_4$; a 2-butyne asymmetric dimer has not been observed.[13]

reminiscent of alkyllithium chemistry,[30] where clusters incorporating lithium halides are quite common. Reduction of $Re(O)I(RC{\equiv}CR)_2$ by sodium metal at −78 °C avoids contamination with naphthalene, but does not avoid the NaI byproduct. Also, the reaction must be kept at −78 °C during its entire course to prevent reaction of $Re(O)I(RC{\equiv}CR)_2$ with 1 to give dimers, which are not reduced further under these conditions.

The best preparative route to compounds 1 in our hands is reduction of the dimers with Na metal and a catalytic amount of naphthalene (usually 1–2%) in THF. No naphthalene is detectable by ^1H NMR and IR after solvent removal *in vacuo*. This synthesis is conveniently carried out at ambient temperatures, especially for **1a** and **1b**.[31] NaI contamination is avoided by chromatographic purification of the dimers prior to reduction. If NaI incorporation is unimportant, as in the synthesis of $ReI(RC{\equiv}CR)_3$,[22] 1 can be prepared by reduction of $Re(O)I(RC{\equiv}CR)_2$ with excess Na/catalytic naphthalene.

The anions 1 are highly reactive and darkly colored compounds (**1a**, **1b**, deep orange; **1c**, red-purple), unlike the other rhenium–oxo–bis(acetylene) compounds such as $Re(O)I(RC{\equiv}CR)_2$ and $Re_2O_2(RC{\equiv}CR)_4$ which are white or yellow and relatively inert. The anions are strong bases and strong nucleophiles. Protonation and reaction with carbon electrophiles such as methyl iodide and acetyl chloride results in addition of H^+ or R^+ to the rhenium, forming oxo–hydride, oxo–methyl, oxo–acyl, and other compounds.[14] Compounds **1a** and **1b** deprotonate stoichiometric acetone, water, and alcohols in acetonitrile solution. With trimethylsilyl reagents, attack occurs at the oxo group, with formation of the siloxide–tris(acetylene) compounds $Re(OSiMe_3)(RC{\equiv}CR)_3$.[22] The anions 1 are also very readily oxidized to the dimers, for instance by dry air, ^{t}BuI, PhI, Cp_2Fe^+, and even Cp_2Co^+ (Scheme 1).[14] **1a** and **1c** also react with the oxygen-atom-transfer oxidant pyridine *N*-oxide, giving free pyridine, 0.5 equiv of the free acetylene, and apparently paramagnetic rhenium product(s). Similar results are seen with Me_2SO, N_2O, pure O_2, and $PhNO_2$. Oxygen-atom acceptors and potential ligands such as PPh_3 or pyridine do not react with 1.

The exchange of bound acetylene ligands is observed upon addition of PhC≡CPh to **1a** in CD_3CN (eq 1); an intermediate is observed by NMR (possibly the mixed acetylene complex) as well as another uncharacterized phenyl product. There is no apparent reaction of **1c** with 2-butyne, indicating that the ReO^- fragment prefers PhC≡CPh to MeC≡CMe. There is also no reaction of **1a** with 2-butyne or **1c** with PhC≡CPh, although **1a** reacts with MeC≡CH to yield a variety of products.

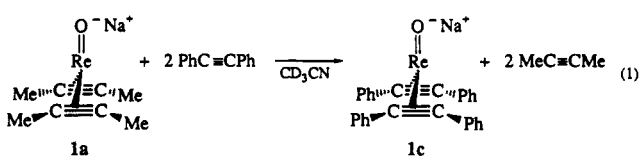

(1)

The high reactivity of 1 has frustrated most of our attempts at exchanging the sodium ion to another cation with a lower tendency to ion pair. For instance, **1a** reacts

(30) Setzer, W. N.; Schleyer, P. v. R. *Adv. Organomet. Chem.* **1985**, *24*, 353.

(31) Caution should be exercised, however, particularly with **1c**, as it appears that over-reduction can take place to produce black uncharacterized solids.

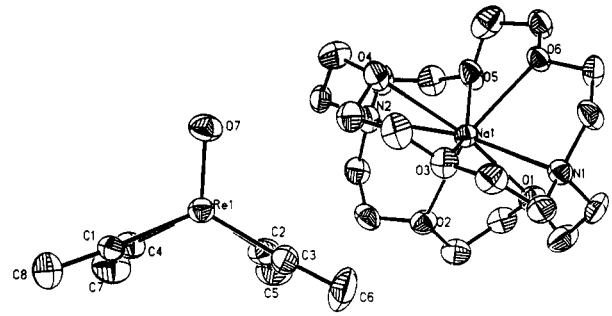

Figure 1. ORTEP drawing of one anion and one cation in the structure of $[Re(O)(MeC{\equiv}CMe)_2][Na(crypt)]$ (**1a**·crypt).

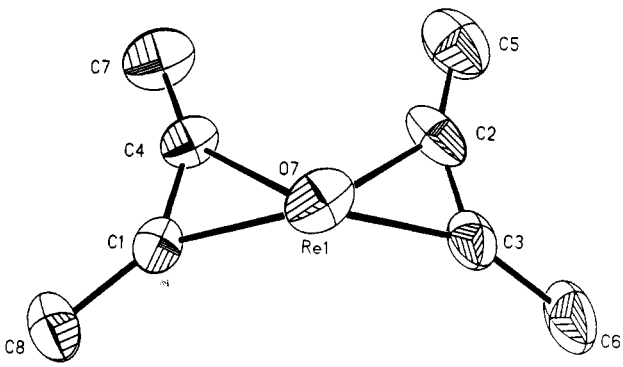

Figure 2. ORTEP drawing of the anion in the structure of $[Re(O)(MeC{\equiv}CMe)_2][Na(crypt)]$ (**1a**·crypt) looking down the Re–O vector; the rhenium atom is obscured by the oxygen.

with Me_4N^+, $^nBu_4N^+$, and PPN^+ ($Ph_3PNPPh_3^+$) cations, in the last case yielding some Ph_3P by NMR. In addition, incomplete cation metathesis and NaX precipitation is often observed. In one case, a vial containing **1a** and the cryptand 4,7,13,16,21,24-hexaoxa-1,10-diazabicyclo[8.8.8]-hexacosane (Kryptofix 222) deposited crystals of $[Re(O)(MeC{\equiv}CMe)_2][Na(crypt)]$ over a year in the freezer in the dry box (see below), but this material has not been isolated in quantity.

B. Structures and Spectra. The X-ray crystal structures of $[Re(O)(MeC{\equiv}CMe)_2][Na(crypt)]$ (**1a**·crypt) and $[Re(O)(PhC{\equiv}CPh)_2Na(MeCN)_2]_2$ (**1c**·2MeCN) both contain a rhenium center coordinated only to one oxo group and two acetylene ligands (Figures 1–4; Table 3). In **1a**·crypt, there are discrete $Re(O)(MeC{\equiv}CMe)_2^-$ anions and $Na(crypt)^+$ cations (Figure 1). In contrast, the sodium ions in **1c**·2MeCN bind tightly to the oxo groups of two different $Re(O)(PhC{\equiv}CPh)_2^-$ units in a centrosymmetric dimer (Figure 3). The distorted tetrahedral coordination at sodium is completed by two acetonitriles.

The $Re(O)(MeC{\equiv}CMe)_2^-$ and $Re(O)(PhC{\equiv}CPh)_2^-$ anions in the two structures are remarkably similar, given the differences in the acetylene substituents and the Na–O interactions. All of the corresponding rhenium–ligand bond distances in the two structures are the same within the estimated uncertainties: for instance, the Re–O distances are 1.745(7) and 1.756(3) Å. The largest difference in corresponding bond lengths is 0.018 Å, in a rhenium–carbon distance. The corresponding angles involving the rhenium are also very similar, with the largest difference being 3.8° in one of the C–Re–C angles (in **1a**·crypt, C(1)–Re(1)–C(3) = 127.7(4)°; in **1c**·2MeCN, C(2)–Re–C(3) = 123.9(2)°). Because the structures are so similar, the description that follows will use the metrical data from the isolated anion in **1a**·crypt.

The rhenium–oxo–bis(acetylene) anions have a non-

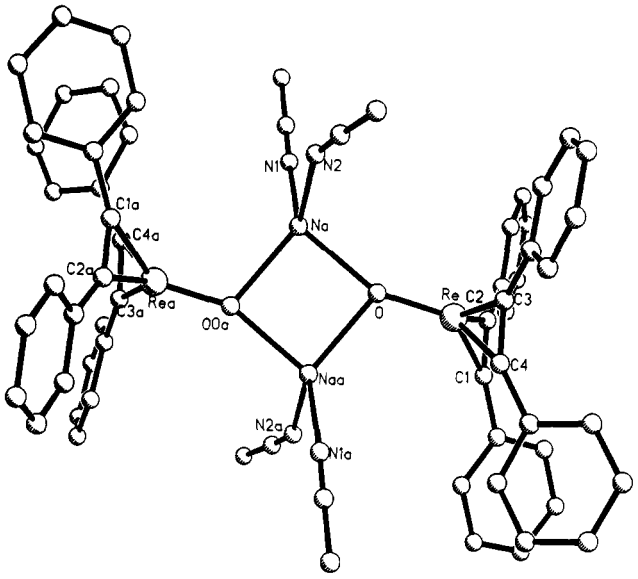

Figure 3. Drawing of the centrosymmetric dimer [Re(O)-(PhC≡CPh)$_2$Na(MeCN)$_2$]$_2$ (**1c**·2MeCN).

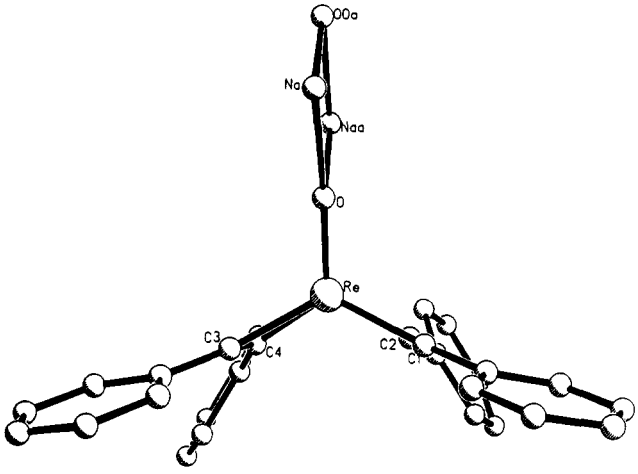

Figure 4. Drawing of [Re(O)(PhC≡CPh)$_2$Na(MeCN)$_2$]$_2$ (**1c**·2MeCN) showing a portion of the centrosymmetric dimer, omitting the acetonitriles bound to sodium and the rhenium center and its acetylene ligands attached to the top oxygen atom.

crystallographic mirror plane that relates the two acetylene ligands (evident in Figures 2 and 4). The acetylenes lie roughly perpendicular to the rhenium–oxo bond so the anions can be described as a distorted square-based pyramid, counting the four acetylene carbons as the corners of the square. The acetylenes are not parallel, however, but are splayed, such that there is an "open" end of the molecule. The "square base" of the coordination sphere is therefore a trapezoid. This is a significant distortion: the C–Re–C angle at the open end is 127.7(4)° versus 90.1-(5)° at the other end (the difference in angels is a little smaller for **1c**·2MeCN (123.2(9)° versus 91.7(2)°), possibly because of the larger acetylene substituents). In addition, the trapezoid base is not quite perpendicular to the Re–O bond because the O–Re–C angles are smaller to the carbons toward the open end (112.5(3)° and 115.0(3)° versus 125.4-(5)° and 124.4(3)°). The angle between the best plane described by the acetylene carbons and the Re–O bond is 73.4°.

The unusual splaying of the acetylenes appears to be electronic in origin rather than due to intramolecular steric effects or packing forces. The same distortion is observed in the sterically very different structures of **1a**·crypt and **1c**·2MeCN, and the distortion is reproduced in the ECP calculations (see below). In addition, a very similar structure is observed for the bulky imido analog, Re(NAr)-(NpC≡CNp)$_2$Na(THF)$_2$ (Ar = 2,6-C$_6$H$_3$^{i}Pr$_2$; Np = CH$_2$-CMe$_3$),[16] in which the sodium ion is coordinated to the imido nitrogen. This displays an almost identical splaying of the acetylenes, with C–Re–C angles of 128.7(4)° and 90.4(4)° at the open and closed ends of the molecule.

The splaying of the acetylenes makes the anions **1** closely resemble their synthetic precursors, Re(O)I(RC≡CR)$_2$ (**2**,[10] Scheme 1), except for the absence of the iodide ligand: the similarity in the metrical data (Table 3) is remarkable. The acetylenes are only very slighlty less splayed in **1a**·crypt than in **2a** (<C–Re–C = 127.7(4)°, 90.1(5)° in **1a** vs 130.5(2)°, 88.3(2)° in **2a**). The acetylene ligands bend a little more away from the oxo group in the anions: the O–Re–C angles average 119.3° in **1a**·crypt vs 111.7° in **2a**. The plane defined by the acetylene carbons is closer to perpendicular to the Re–O bond in **2a**, and the slight tilt is opposite to that found in **1a**·crypt, with the carbons toward the open end bent away from the oxygen in **2a** (115.0(3)° at the open end vs 109.1(2)° on the other side).

In sum, two-electron reduction of **2a** causes little structural change. The bond lengths in **1** vs **2** are therefore directly comparable. The rhenium–oxygen bond gets 0.05 Å longer on reduction, as the bond lengths in the anions are 1.745(7) and 1.756(3) Å vs 1.70 Å for a variety of Re-(O)X(RC≡CR)$_2$ derivatives.[32] While 0.05 Å is not a large change, it does suggest a significant difference in bond order: a statistical survey of rhenium–oxo distances suggested that Re–O triple bonds average 1.686 Å while double-bond distances average 1.761 Å (for octahedral trans-d^2-dioxo species) or 1.708 Å (for d^0 trioxo and tetraoxo complexes).[33] The rhenium–carbon distances are slightly shorter in the anions than in **2a** (average 2.005 Å in **1a**·crypt, 2.051 Å in **2a**). This reflects the stronger back-bonding in the electron-rich anions (see below), consistent with the apparently slightly longer C≡C distances. In the anions, the two Re–C bonds at the open end are slightly shorter than the other two, while the opposite is true for **2a** (Table 3).

Infrared and NMR spectra provide an additional comparison between **1** and **2**. The rhenium–oxygen stretching frequencies observed for **1**, 805–840 cm^{-1}, are much lower than found for **2** (970–980 cm^{-1} for the halide derivatives and similar for other Re(O)X(RC≡CR)$_2$ compounds[34]). For **1c**, the Re–O stretch at 824 cm^{-1} shifts to 763 cm^{-1} on ^{18}O substitution. When **1c** is isolated in the presence of 18-crown-6, ν_{ReO} appears at 885 cm^{-1}. For **1a** and **1b**, two bands likely due to ν_{ReO} are observed (at 835, 805 cm^{-1} for **1a** in a Nujol mull, and at 840, 810 cm^{-1} for **1b** as a neat oil), possibly because of formation of ion-paired clusters. The IR spectrum of **1a**·crypt displays a single band at 869 cm^{-1} tentatively assigned as ν_{ReO}; **1b** isolated in the presence of 18-crown-6 shows bands at 870 and 860 cm^{-1}. Thus, removal of the sodium cation by coordination to an added ligand raises the rhenium–oxygen

(32) See refs 10, 11, 13, and the following: (a) Erikson, T. K. G.; Bryan, J. C.; Mayer, J. M. *Organometallics* **1988**, *7*, 1930. (b) Mayer, J. M.; Tulip, T. H.; Calabrese, J. C.; Valencia, E. *J. Am. Chem. Soc.* **1987**, *109*, 157.

(33) Mayer, J. M. *Inorg. Chem.* **1988**, *27*, 3899. Bond orders are derived from simple molecular orbital and symmetry arguments.

(34) References 10, 11, 13, 14, 32a,b, and the following: Erikson, T. K. G.; Mayer, J. M. *Angew. Chem., Int. Ed. Engl.* **1988**, *27*, 1527.

Chart 1

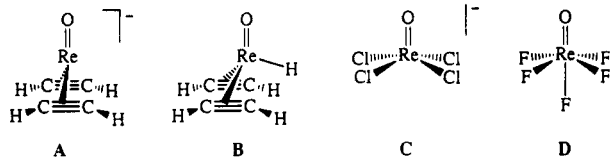

A B C D

stretching frequency, consistent with the suggestion of strong Na–O interactions. Even with an encapsulated sodium ion, however, the stretching frequencies are ca. 100 cm^{-1} lower in the anion than in **2**, again indicative of a lower Re–O bond order for the anion.

The acetylenic stretches, observed as weak bands in the spectra of both **1** and **2**, are again lower in the anions: 1685 and 1690 cm^{-1} for **1a** and **1b** vs 1800 and 1780 cm^{-1} for **2a** and **2b**. Small further decreases in $\nu_{C\equiv C}$ are observed on addition of crypt to **1a** (from 1685 to 1675 cm^{-1}) and on addition of crown to **1c** (from 1665 to 1660 cm^{-1}). These values indicate greater back-bonding from the rhenium center to the acetylenes in the anions compared to **2**, as suggested above on the basis of structural data. Removal of the sodium from the anions presumably makes the anions slightly more electron rich, increasing the back-bonding.

The NMR spectra of **1a–c** display a single resonance for the acetylenic carbons and a single set of resonances for the four acetylene substituents. Thus **1a** shows a single peak in the ^1H NMR at δ 2.74, due to four equivalent methyl groups, and two resonances in the ^{13}C NMR, at δ 19.9 ($CH_3C\equiv CCH_3$) and 166.3 ($C\equiv C$). In **1b**, the methylene hydrogens are diastereotopic. The data are not consistent with the static (C_S) structure with splayed acetylenes found in the solid state (and computationally, see below), in which the ends of each acetylene are inequivalent. The spectra indicate either a static C_{2v} structure or, more likely, that the anions are fluxional, interconverting C_S ground-state structures. The simplest such motion is a rocking of the acetylene ligands back and forth through a C_{2v} structure, as illustrated in eq 2 looking down the O–Re bond (the same view as in Figure 2). No splitting of the acetylene signals is observed in the ^1H NMR of **1a**·crypt down to 200 K in d_8-THF. The acetylenic ^{13}C chemical shifts for compounds **1** are in the range δ 166–173, slightly downfield of the signals for **2a–c**, δ 138–148, but still in the range of three-electron donor alkynes.[35]

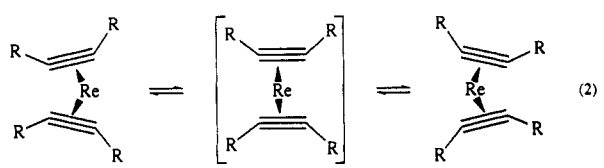

(2)

II. Computational Studies. A. Geometry of Rhenium–Oxo Complexes. Effective core potential (ECP) methods have been used to calculate the geometry and bonding in rhenium–oxo anions **1**, together with a number of other rhenium–oxo compounds for comparison (Chart 1). The wide range of metal formal oxidation states in which rhenium–oxo complexes can be found provides an interesting opportunity to further test the predictive capacity of ECP methods for transition metal chemistry.

(35) Templeton, J. L.; Ward, B. C. *J. Am. Chem. Soc.* **1980**, *102*, 3288–90. Templeton, J. L. *Adv. Organomet. Chem.* **1989**, *29*, 1–100.

Table 4. Comparison of Calculated and Experimental Geometries for Rhenium–Oxo Complexes[a]

	$Re(O)F_5$		$Re(O)Cl_4^-$		
Re–O, Å	1.63	1.642(10)	Re–O, Å	1.62	1.627(24)
$Re–F_{cis}$, Å	1.82	1.810(7)	Re–Cl, Å	2.39	2.344(4)
$Re–F_{trans}$, Å	1.88	nr[b]	O–Re–Cl, deg	106	100.0(5)
$O–Re–F_{cis}$, deg	95	93.1(2)			

	$Re(O)H(HCCH)_2$ (calcd)[c]	$Re(O)I(MeCCMe)_2$ (exptl[10])
Re–O, Å	1.66	1.697(3)
$Re–C_A$, Å	2.06	2.061(5), 2.066(5)
$Re–C_B$, Å	2.06	2.038(5), 2.040(5)
$C_A–C_B$, Å	1.30	1.278(7), 1.288(7)
$O–Re–C_A$, deg	115	114.8(2), 114.2(2)
$O–Re–C_B$, deg	114	109.1(2), 108.8(2)
Re–H[d], Å	1.66	*d*
O–Re–H[e], deg	109	109.4(1)[e]

	$[Re(O)(HCCH)_2]^-$ (calcd)		$[Re(O)(MeCCMe)_2]$ [Na·crypt](**1a**·crypt, exptl)
	C_{2v}	C_s	
Re–O, Å	1.70	1.71	1.745(7)
$Re–C_A$, Å	2.06	2.04	1.976(10), 1.999(11)
$Re–C_B$, Å	2.06	2.05	2.014(10), 2.030(10)
$C_A–C_B$, Å	1.33	1.33	1.287(13), 1.302(17)
$O–Re–C_A$, deg	120	124	124.5(5), 124.2(3)
$O–Re–C_B$, deg	120	114	112.5(3), 115.0(4)

[a] Calculated geometries were determined at the RHF level using effective core potentials and valence basis sets as described in Computational Methods. The calculated minima for $Re(O)F_5$ and $Re(O)Cl_4^-$ are C_{4v}; the calculated minima for the bis(acetylene) complexes are C_s. The C_{2v} structure was obtained from a symmetry-constrained optimization and is a transition state, whose imaginary frequency is described in the text. [b] Not reported. [c] The atoms denoted C_A and C_B represent the symmetry equivalent pairs in the C_s minima which are proximal and distal, respectively, with respect to the hydrido ligand (iodo in the experimental model) and "open" end in the anion. [d] The Re–H distance in $[ReH_9]^{2-}$ is 1.68(1) Å: Cotton, F. A.; Wilkinson, G. *Advanced Inorganic Chemistry*, 5th ed.; Wiley: New York, 1988; p 1108. [e] The experimental value is the O–Re–I angle in $Re(O)I(MeCCMe)_2$.

Agreement between the calculated structures and experimental crystallographic data is excellent: a comparison of pertinent bond lengths and angles between the calculated and observed geometries is presented in Table 4. The calculated minima for the Re(V) and Re(VII) compounds **C** and **D** are C_{4v}, as found experimentally and as is typical of five- and six-coordinate oxo complexes with d^0 or d^2 configurations.[3c] The rhenium–oxo–bis(acetylene) complexes **A** and **B** are calculated to have C_S minima, as observed for **1a**·crypt, **1c**·2MeCN, and **2a** (see above). Metric data for the calculated minimum of **A**, the model for the anions, is given in Figure 5 as well as in Table 4.

A constrained C_{2v} geometry for **A** (the putative transition state for the acetylene rocking motion, eq 2) was also isolated on the $[Re(O)(HC\equiv CH)_2]^-$ potential energy surface, Figure 5. The C≡C bonds are parallel to each other, and both C≡C bonds are perpendicular to the vector which describes the rhenium-oxo bond, as required by C_{2v} symmetry. This C_{2v} stationary point is *not* a minimum on the molecular potential energy surface, but rather a transition state with a calculated imaginary frequency of 152*i* cm^{-1}, which lowers the symmetry to C_S. The imaginary mode for the C_{2v} transition state shows a combination of several motions. First, there is a splaying of the acetylenes which causes one nonbonded C···C distance to increase while the other nonbonded C···C distance decreases (see above). There is also a conrotatory movement of acetylene fragments about an axis connecting the Re atom and the C≡C bond midpoints, so that the

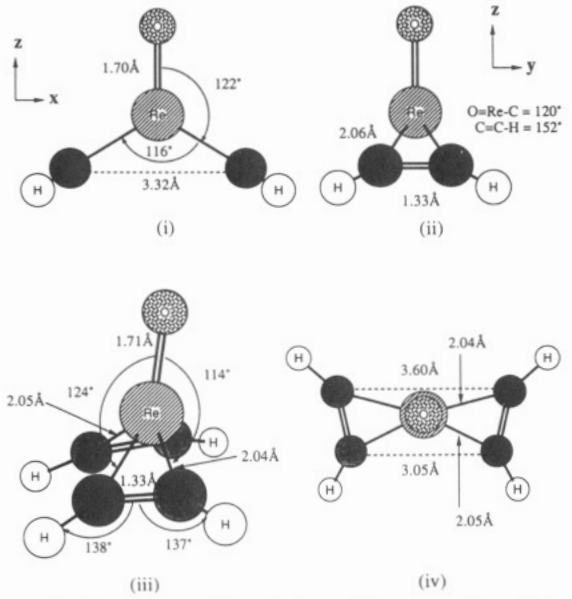

Figure 5. Two views of the C_{2v} transition state (i and ii) and the C_s minimum (iii and iv) geometries of $[Re(O)(HC{\equiv}CH)_2]^-$ calculated using effective core potential methods.

C≡C bonds are no longer perpendicular to the Re=O axis. Finally, the rhenium moves into the "open" region where the two nonbonded carbon atoms are moving apart.

Distortion of the C_{2v} transition state along the imaginary frequency, followed by reoptimization, leads to the C_S minimum (Figure 5). The C_{2v} and C_S structures have identical bond lengths but substantially different bond angles (Table 4). All the changes indicated by the imaginary mode of the C_{2v} structure (see above) have manifested themselves in the calculated minimum, i.e., splaying, acetylene rotation, and pyramidalization of the Re coordination environment. The rhenium is 0.09 Å out of the plane described by the O atom and the C≡C bond midpoints in the C_S minimum, as found in the structure of **1a**·crypt (experimentally, 0.15 Å; Figure 2). The optimized C_S geometry for $[Re(O)(HC{\equiv}CH)_2]^-$ is thus in excellent agreement with the X-ray crystal structure of $[Na(crypt)][Re(O)(MeC{\equiv}CMe)_2]$ (Table 4) in both the bond lengths and angles. Close agreement between calculated and experimental structures has been seen in previous studies of alkylidene ($L_nM{=}C(R)R'$) and imido complexes ($L_nM{=}NR$),[17] and it is encouraging to find it in their oxo cousins.[36]

The C_S minimum is only 2.1 kcal/mol lower in energy than the C_{2v} transition state at the RHF level (7.6 kcal mol^{-1} lower at the MP2 level,[37] using RHF geometries). Adding zero point energy corrections and taking into account the enthalpy change upon going from absolute zero to 298 K, the energy difference between the C_{2v} transition state and the C_S minimum is estimated to be 1.4 kcal mol^{-1} at the RHF level. The calculations suggest that the crystallographically observed acetylene splaying and other distortions from C_{2v} symmetry are due to subtle electronic factors and do not arise from either crystal packing forces or bonding considerations induced by bridging Na^+ counterions. The ability of the present ECP scheme to reproduce these subtle geometric changes in all respects is impressive. The small calculated enthalpy difference between the C_{2v} and C_S geometries is consistent with the solution NMR spectra which indicate C_{2v} symmetry on the NMR time scale to 200 K (see above).

B. Bonding in Rhenium–Oxo Complexes. The bonding in the high-valent C_{4v} complexes $Re(O)Cl_4^-$ and $Re(O)F_5$ (**C** and **D**, respectively) follows the standard framework first enunciated by Ballhausen and Gray.[7c] The d orbital splitting is the familiar "3 under 2" for octahedral complexes with the added factor that the dπ orbitals (d_{xz} and d_{yz} in the present case where the metal–oxo bond lies along the *z*-axis) are moved to higher energy (relative to d_{xy}) due to antibonding mixing in of O pπ. Removal of the trans ligand to yield a square pyramidal structure does not modify the essential nature of the lower-energy d orbitals, so a square pyramidal, d^2 oxo complex such as $Re(O)Cl_4^-$ can fully populate the d_{xy} level without occupying orbitals with Re–O π antibonding character. Plotting the valence molecular orbitals for **C** and **D** does not reveal any MOs with antibonding character between the Re and O atoms. In addition, the calculated intrinsic stretching Re–O frequencies for **C** and **D** are quite similar, 1097 and 1120 cm^{-1}, supporting the nonbonding nature of the occupied d orbital in **C**. The experimental stretching frequencies are 1067 cm^{-1} in $[ReOCl_4][AsPh_4]$[19] and 992 cm^{-1} in $ReOF_5$.[38] (Stretching frequencies for main-group bonds calculated by *ab initio* methods are typically 10% too high, due to correlation and anharmonicity effects.[39] The values reported here have been scaled by the empirical factor of 0.9.)

The bis(acetylene) complexes **A** and **B** are more difficult to analyze than the d^0 and d^2 analogs **C** and **D** due to significant delocalization of the frontier molecular orbitals over the rhenium, the oxygen, and the acetylene ligands. Extended Hückel calculations also indicate delocalization of the frontier MOs for $Re(O)H(HC{\equiv}CH)_2$ and $[Re(O)(HC{\equiv}CH)_2]^-$[10,12] and their imido analogs.[16] This contrasts with the situation for **C** and **D**, in which there is little mixing between the Re–O based MOs and orbitals on the halide ligands. The $Re(O)X(HC{\equiv}CH)_2$ complexes were described, based on the extended Hückel analysis,[10] as tetrahedral $M(O)L_3$ complexes, with the tetrahedral "2 under 3" d orbital splitting reinforced by the metal–oxygen and metal–acetylene π interactions. This provides a satisfying explanation for the unusual stability of the formally d^4 complexes, as orbitals which are Re–O π antibonding are not populated. The ECP wavefunction for $Re(O)H(HC{\equiv}CH)_2$ supports this analysis: plotting molecular orbitals for $Re(O)H(HC{\equiv}CH)_2$ reveals no filled metal–oxygen antibonding MOs.

In studying the Re(I) anion, we have concentrated on the C_{2v} structure since there is only a small enthalpy difference between it and the C_S minimum and the higher symmetry assists in analysis. If the description for the Re(III)–oxo complexes as being $M(O)L_3$ species provides a ready explanation of their bonding, it is reasonable that an understanding of the deprotonated species might commence from an $M(O)L_2$ starting point. The energy ordering of the d orbitals, as derived from ECP calculations

(36) More extensive studies of transition metal oxo complexes are currently underway in our laboratories. Benson, M. T.; Cundari, T. R.; Nguyen, H. D.; Lim, S. J.; Pierce-Beaver, K. *J. Am. Chem. Soc.*, submitted for publication.

(37) Moller–Plesset second-order perturbation theory. Moller, C.; Plesset, M. S. *Phys. Rev.* **1934**, *46*, 618.

(38) Bartlett, N.; Jha, N. K. *J. Chem. Soc. A* **1968**, 536–43.

(39) Pople, J. A.; Schlegel, H. B.; Krishnan, R.; DeFrees, D. F.; Binkley, J. S.; Frisch, M. J.; Whiteside, R.; Hout, R. F.; Hehre, W. J. *Int. J. Quantum Chem., Proc. Sanibel Symp.* **1981**, *15*, 269. An examination of calculated vs observed metal–oxo stretching frequencies has, to our knowledge, not been reported but is underway in our laboratory.[36]

Scheme 2. Energy levels in $[Re(O)(RC{\equiv}CR)_2]^-$ (1) near the HOMO, with the Primary Rhenium Orbital Components Indicated

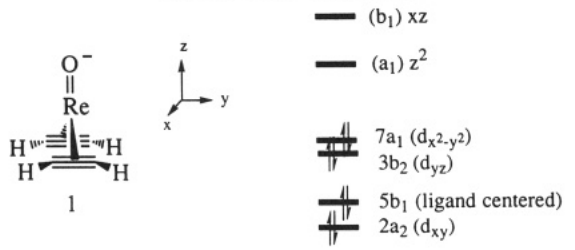

1

and shown in Scheme 2, is intuitively reasonable from this perspective. The four highest occupied molecular orbitals are $2a_2$, $5b_1$, $3b_2$, and $7a_1$ (from lowest to highest energy). The $2a_2$ is the Re d_{xy} orbital stabilized by π-back-bonding to the acetylene ligands (using Dewar–Chatt–Duncanson terminology); in fact it is an equal mixture of the Re d_{xy} and the appropriate symmetry-adapted linear combination of HC≡CH π^* orbitals. The $7a_1$ (the HOMO) is nearly all Re $d_{x^2-y^2}$ in character with a small contribution from the acetylene ligands. Previous extended Hückel calculations[12] predicted the HOMO to be $3b_2$ rather than $7a_1$, although the energy difference between these MOs is calculated here to be only 0.8 eV.

The $5b_1$ orbital is ligand-centered, as depicted schematically in the xz plane, mostly acetylene $\pi_{C\equiv C}$ with a small (11%) O p_x contribution.

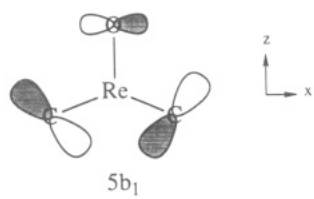

$5b_1$

A similar ligand-centered orbital has been seen in the electronic structure of other complexes with pseudo-3-fold symmetry and potentially π-bonding ligands, including $W(CO)(RC{\equiv}CR)_3$, $Os(NAr)_3$, $W(NR)(OSiR_3)_2$, and $[Re(NAr)_n(RC{\equiv}CR)_{3-n}]^-$.[40] In complexes with full 3-fold symmetry, this orbital has a_2 symmetry and finds no metal orbital of like symmetry with which to interact. The pseudotetrahedral complex $Re(O)H(HC{\equiv}CH)_2$ (**B**) also has an acetylene-based nonbonding orbital, quite similar to $5b_1$ except without a significant oxygen component. An acetylene-based nonbonding orbital is consistent with the conclusions from NMR studies of $NaRe(O)(RC{\equiv}CR)_2$ (1) and $Re(O)X(RC{\equiv}CR)_2$ compounds (see above and ref 10) that each acetylene behaves as a three-electron donor. The orbital drawn as $5b_1$ can thus be considered as the receptacle for the seventh and eighth π electrons of the two acetylene ligands.

The $3b_2$ is perhaps the most interesting molecular orbital. It is a combination of the Re d_{yz} orbital with all three of the ligands: the interaction with the acetylene π^* orbitals is in-phase (a π-back-bonding interaction) while the O p_y is mixed in so as to be π-antibonding, as shown below.

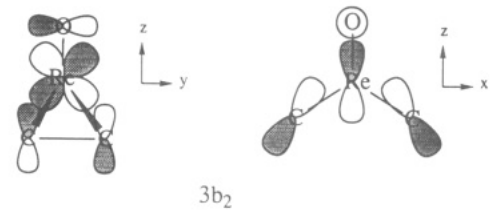

$3b_2$

The ECP calculations and a Mulliken population analysis[41] partition $3b_2$ as follows: 22% Re, 13% O, and 16% per acetylene C. Using the Fenske–Hall program[42] to partition the molecular orbitals of **A** into ReO^- + $(HC{\equiv}CH)_2$ fragments generates a description of the $3b_2$ molecular orbital as 14% ReO π + 36% ReO π^* + 48% $(HC{\equiv}CH)_2$ π^*.

The driving force for the distortion from C_{2v} to C_S $[Re(O)(HC{\equiv}CH)_2]^-$ is difficult to analyze from an orbital perspective because of the low symmetry. The largest change on distortion is the lowering in energy of the $3b_2$ orbital, but the origin of this stabilization is complicated by mixing of $3b_2$ with $7a_1$ (both MOs become a′). The other frontier molecular orbitals that change in both energy and composition, the $5b_1$, $2a_2$, and $4b_1$[43] orbitals, all become a″ upon distortion and mix, although as a group their net energy change appears to be small. A detailed interpretation of these changes does not appear to be warranted, given the very small energy differences involved.

III. Connection of the Electronic Structure with the Chemistry of $[ReO(RC{\equiv}CR)_2]^-$. Reduction of $Re(O)I(RC{\equiv}CR)_2$ compounds (**2**) by two electrons results in loss of I^- and formation of $[ReO(RC{\equiv}CR)_2]^-$ (1). The metal-based molecular orbitals in the formally d^4 complexes **2** are expected to be d_{xy} and $d_{x^2-y^2}$ on the basis of a qualitative molecular orbital analysis.[10] This general conclusion is supported by the ECP calculations although there is significant delocalization among the metal and ligand orbitals. The two electrons added to **2** occupy an orbital with significant Re d_{yz} character, specifically $3b_2$ in the C_{2v} symmetry we have used to analyze the electronic structure of **1**. The loss of I^- on reduction is consistent with the Re–I σ^* character of the Re d_{yz} orbital in **2**. Addition of two electrons also leads to much greater back-bonding in **1** (modeled by **A**) than in **2** (**B**). In **B**, the calculated total charge on the two acetylenes is +1.04 so that, in Dewar–Chatt–Duncanson terms, σ-donation dominates over back-bonding. In **A**, however, the charge on the two acetylenes is −0.08, indicating that back-bonding is much more significant relative to σ-donation for the anion.

Compounds **1** are surprisingly stable as monomeric species with rhenium–oxygen multiple bonds and do not oligomerize to compounds with μ-oxo bridges. For most metal–oxo complexes, population of metal–oxygen π^* orbitals leads to μ-oxo compounds or other species derived from Lewis acid attack at the oxo group.[3c,9] In the μ-oxo and related compounds, π-antibonding interactions are much reduced. The stability of the formally d^6 rhenium–oxo anions **1** is likely due in part to delocalization of the Re–O π^* electron density onto the acetylenes by the back-

(40) (a) $W(CO)(RC{\equiv}CR)_3$: King, R. B. *Inorg. Chem.* **1968**, *7*, 1044–6. (b) $Os(NAr)_3$: Kee, T. P.; Anhaus, J. T.; Schrock, R. R.; Johnson, K. H.; Davis, W. M. *Inorg. Chem.* **1991**, *30*, 3595. (c) $W(OSi^tBu_3)_2(N^tBu)$: Eppley, D. F.; Wolczanski, P. T.; Van Duyne, G. D. *Angew. Chem., Int. Ed. Engl.* **1991**, *30*, 584. (d) $[Re(NAr)_3]^-$, $[Re(NAr)_2(RC{\equiv}CR)]^-$, and $[Re(NAr)(RC{\equiv}CR)_2]^-$: Reference 16.

(41) Mulliken, R. S. *J. Chem. Phys.* **1955**, *23*, 1833, 1841, 2338, 2343.

(42) Hall, M. B.; Fenske, R. F. *Inorg. Chem.* **1972**, *11*, 768. Version 5.1, kindly provided to T.R.C. by Prof. Michael B. Hall, Texas A & M. Standard program parameters were used to transform from an AO to an MO basis.

(43) The $4b_1$ orbital is similar to ligand-centered $5b_1$ except with greater metal contribution and with the opposite phase of the O p_x orbital, so it has Re → acetylene back-bonding and Re–O bonding character.

bonding interaction in the $3b_2$ orbital. The recently reported "pogo stick" imido complexes Cp*Ir(NR)[44] and (Arene)Os(NR)[45] are in one sense isoelectronic with **1**, as the metals are also d^6 and the Cp^{*-} or arene ligand donates three electron pairs to the metal as do the two acetylene ligands in **1**. (Note that the related oxo complex is dimeric, $Cp^*Ir(\mu\text{-}O)_2IrCp^*$.[46]) The iridium and osmium compounds do not appear to populate any orbitals with π^* character, however, as the six d electrons are accommodated in the d_{xy}, $d_{x^2-y^2}$, and d_{z^2} orbitals.[47] In **1**, the Re d_{z^2} orbital is not available as it is strongly bonding with the $\pi_\perp$ orbital of the acetylene ligands, so that the $3b_2$ orbital involving Re d_{yz} is populated.

The reaction chemistry of compounds **1** is dominated by their strong reducing power, their high nucleophilicity, and their high basicity.[12,14,22] All three properties are rationalized by the presence of high-energy, metal-centered molecular orbitals, $7a_1$ and $3b_2$. The regiochemistry of attack at compounds **1** varies with the electrophile. Protonation and alkylation seem to be orbitally controlled because attack occurs at rhenium.[14] Electrophilic attack could occur at either high-energy orbital; $7a_1$ is the HOMO, but attack at $3b_2$ (only 0.8 eV lower in energy) would directly lead to the ground state of the tetrahedral products, $Re(O)R'(RC{\equiv}CR)_2$. In contrast, silicon electrophiles[22] and the sodium cations in the structure of $(\mathbf{1c}\cdot 2MeCN)_2$ bind to the oxo ligand, apparently because these are charge-controlled processes. The ECP calculations support this picture, as they indicate net charges of –0.85 at the oxygen, –0.2 at the acetylene carbons, and –0.07 at rhenium in **A**.

On the basis of the nodal structure of $3b_2$, occupation of this orbital should weaken the rhenium–oxygen bond. The Re–O bond length in $[Re(O)(HC{\equiv}CH)_2]^-$ (**A**) is calculated to be 0.05 Å longer than that in $Re(O)H(HC{\equiv}CH)_2$ (**B**), the same difference as found experimentally between Re–O bonds in $[Na(crypt)][Re(O)(MeC{\equiv}CMe)_2]$ and $Re(O)I(MeC{\equiv}CMe)_2$. The stretching frequencies also indicate weakening of the Re–O bond on reduction, from 975 cm^{-1} in **2a** (calculated 1012 cm^{-1} in **B**) to 869 cm^{-1} in **1a**·crypt (calculated 905 cm^{-1} for **A**). The large changes in the Re–O bond on reduction are interesting, given that the key $3b_2$ orbital has only partial Re–O π^* character. In fact this orbital has more rhenium–acetylene back-bonding character than Re–O π^* character (see above). An interesting comparison is presented by octahedral ruthenium(IV)–oxo compounds such as *cis*-$[Ru(O)(bpy)_2py]^{2+}$, which have been suggested to have two electrons in Ru–O π^* orbitals on the basis of ligand-field arguments.[48] This picture has been supported by molecular orbital calculations,[7e] which show little delocalization from the Ru(IV)–oxo fragment to the ancillary ligands. The ruthenium complexes have Ru–O bonds roughly 0.1 Å longer than would be expected if π^* orbitals were not populated[33] and have unusually low stretching frequencies, ca. 800 cm^{-1} compared to the normal range of 900–1050 cm^{-1} for metal–oxo complexes.[49] The magnitude of the changes in the Re–O bond between **1** and **2** is thus roughly half of the effect in the ruthenium case, consistent with only partial π^* character in **1**. These data support the suggestion[9] that population of π^* orbitals has a substantial effect on a metal–oxygen bond.

Acknowledgment. Effective core potential studies of transition metal chemistry at Memphis State are supported by the National Science Foundation (in the form of grants of time on the iPSC/860 at San Diego Supercomputer and the Cray Y-MP at National Center for Supercomputing Applications), Oak Ridge National Laboratories (for access to the iPSC/860 through our collaboration with the Joint Institute for Computational Science at University of Tennessee—Knoxville), IBM (participation in the Developer's Discount program), and the Air Force Office of Scientific Research (Grant No. 93-10105). Rhenium–oxo acetylene chemistry has been generously supported by the National Science Foundation. We thank Dr. David Barnhart for his help with the crystal structure of **1a**·crypt and Dr. David Thorn for his extended Hückel calculations and for his many insights.

Supplementary Material Available: Crystallographic tables for $[Re(O)(MeC{\equiv}CMe)_2][Na(crypt)]$ (**1a**·crypt) and $[Re(O)(PhC{\equiv}CPh)_2Na(MeCN)_2]_2$ (**1c**·2MeCN) (20 pages). Ordering information is given on any current masthead page.

OM930526A

(44) Glueck, D. S.; Hollander, F. J.; Bergman, R. G. *J. Am. Chem. Soc.* **1989**, *111*, 2719. Glueck, D. S.; Wu, J.; Hollander, F. J.; Bergman, R. G. *J. Am. Chem. Soc.* **1991**, *113*, 2041.

(45) Michelman, R. I.; Andersen, R. A.; Bergman, R. G. *J. Am. Chem. Soc.* **1991**, *113*, 5100–2.

(46) McGhee, W. D.; Foo, T.; Hollander, F. J.; Bergman, R. G. *J. Am. Chem. Soc.* **1988**, *110*, 8543. See also: Dobbs, D. A.; Bergman, R. G. *J. Am. Chem. Soc.* **1993**, *115*, 3836–7.

(47) Glueck, D. S.; Green, J. C.; Michelman, R. I.; Wright, I. A. *Organometallics* **1992**, *11*, 4221.

(48) A singlet ground state is found for *cis*-$[Ru(O)(bpy)_2py]^{2+}$ with a low-energy triplet excited state only 56 cm^{-1} higher in energy in solution. These states differ only in the spin coupling of the Ru–O π^* electrons and are both populated at room temperature. Dobson, J. C.; Helms, J. H.; Doppelt, P.; Sullivan, B. P.; Hatfield, W. E.; Meyer, T. J. *Inorg. Chem.* **1989**, *28*, 2200–4.

(49) Reference 3c, pp 116–117.